INSTITUTE OF PHYSICS PUBLISHING and INTERNATIONAL ATOMIC ENERGY AGENCY NUCLEAR FUSION

Nucl. Fusion **46** (2006) 858–863 doi:10.1088/0029-5515/46/10/003

Modelling of stochastic magnetic perturbation by RWMEF coils on NSTX

Longwen Yan[1], T.E. Evans[2], S.M. Kaye[3] and R. Maingi[4]

[1] Southwestern Institute of Physics, PO Box 432, Chengdu, Sichuan 610041, People's Republic of China
[2] General Atomics, PO Box 85608, San Diego, CA 92186-5608, USA
[3] Plasma Physics Laboratory, Princeton University, Princeton, NJ 08543, USA
[4] Oak Ridge National Laboratory, Oak Ridge, TN 37831, USA

E-mail: lwyan@swip.ac.cn

Received 18 April 2006, accepted for publication 31 July 2006
Published 30 August 2006
Online at stacks.iop.org/NF/46/858

Abstract

A 3-D field line integration code, TRIP3D, has been modified to model stochastic magnetic perturbation produced by a resistive wall mode, error field (RWMEF) coil in the NSTX tokamak with very low aspect ratio. Multiple field lines with a uniform poloidal angle interval on each flux surface are automatically traced for the first time to follow the lines with large elongation plasmas. Each RWMEF coil can be configured to produce perturbation fields with dominant toroidal mode numbers of $n = 1$ or 3. In this study, it is found that the strongest stochastic layer is produced by the $n = 3$ configuration rather than $n = 1$ for the same coil current. Two NSTX divertor discharges, a lower single null and a double null have been modelled with different RWMEF-coil currents and toroidal modes. RWMEF currents of 2 kAt are sufficient to produce a strong stochastic field and significantly perturb the plasma boundary due to weak toroidal field in the spherical tokamak. The edge electron thermal diffusivity due to stochastic magnetic field is estimated to be 1 $m^2\ s^{-1}$ with a 2 kAt current, which is comparable to that in DIII-D with an 8 kAt C-coil current. Currents of this magnitude, when used in the DIII-D I-coil configured for $n = 3$ perturbations suppress large edge localized modes (ELMs) and thus may have an impact on ELMs in NSTX. The result has been verified by the initial experiments.

PACS numbers: 52.65.Cc, 52.25.Fi, 52.55.Fa

(Some figures in this article are in colour only in the electronic version)

1. Introduction

NSTX is a low aspect ratio spherical tokamak with parameters [1, 2] $R = 0.85$ cm, $a = 0.68$ m, $A = R/a > 1.25$, $B_t \leqslant 0.6$ T, $I_p \leqslant 1.5$ MA, elongation $\kappa \leqslant 3.0$, triangularity $\delta \leqslant 0.9$, 7.5 MW of NBI and 6 MW RF heating. The H-mode feature has been studied in detail. Especially, the tiny edge localized modes (ELMs) called Type V are often observed [3]. The layout of NSTX is shown in figure 1. Five pairs of poloidal field coils, named PF1–PF5, are used to control the plasma configuration. The resistive wall mode, error field (RWMEF)-coils marked by red vertical lines are installed inside the PF5 coil and located at $R = 1.761$ m with the height of 0.965 m. There are six RWMEF-coil loops on NSTX. The toroidal span angles are 57.3° for No 1, 59.3° for No 2, 59.0° for No 3, 55.7° for No 4, 53.6° for No 5 and 56.2° for No 6. Since each loop consists of two turns, 1 kA of current in the coil results in a perturbation of 2 kAt. Every turn can carry a current of 3 kA. There is approximately up–down symmetry along the midplane for the segments of each coil. The coils are quite close to the last closed flux surface (LCFS) near $R = 1.53$ m. The distance between the coils and the LCFS is 0.23 m in NSTX, while the C-coil [4] in DIII-D is 0.95 m from the LCFS. The edge magnetic perturbation produced by a 1 kAt RWMEF-coil current in NSTX is a little larger than that produced by a 4 kAt C-coil current in DIII-D. Although they are all intended to function similarly, the RWMEF-coils and the DIII-D I-coils are close to the plasma boundary while the DIII-D C-coil is located about 1 m away from the midplane plasma boundary.

2. Modelling for the stochastic magnetic boundary in NSTX

A three-dimensional field line integration code, TRIP3D, was developed to model the stochastic behaviour of the magnetic field near the boundary of toroidal magnetic confinement devices [5]. In the TRIP3D, the unperturbed magnetic field

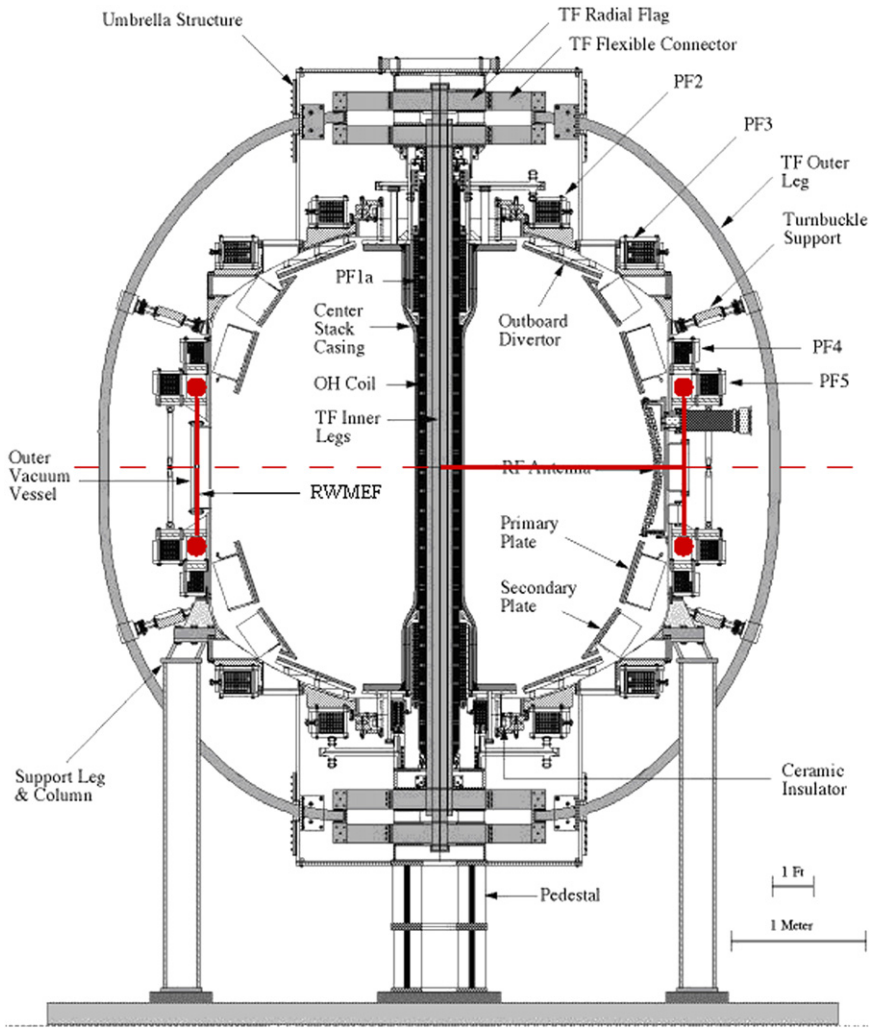

Figure 1. The layout of the NSTX tokamak. The red vertical lines inside PF5 are RWMEF-coils and located at $R = 1.761$ m with the height of 0.965 m. There are six RWMEF-coil loops on NSTX.

(B_R, B_ϕ, B_Z) at each point is provided by the EFIT code [6]. The perturbed field (b_R, b_ϕ, b_Z), produced by RWMEF coil currents, is calculated for each integration step and added to the unperturbed one. To follow the field lines, the code integrates a set of first-order cylindrical (R, ϕ, Z) magnetic differential equations as

$$\frac{\partial R}{\partial \phi} = \frac{R(B_R + b_R)}{B_\phi + b_\phi}, \qquad \frac{\partial Z}{\partial \phi} = \frac{R(B_Z + b_Z)}{B_\phi + b_\phi}. \tag{1}$$

The diffusion coefficient of a stochastic field line is defined as $D_{\rm st} = \delta r^2/2L$, where δr is radial step in minor radius and L is the field line length. Recently, TRIP3D was modified to calculate field line integrals starting at different poloidal angles on the same unperturbed flux surface. Here, the radial step is replaced by the normalized magnetic flux step to describe the magnetic diffusion coefficient with so-called long path integrals and the flux space diffusion coefficient is defined as $\langle D_{\rm st}^{\psi} \rangle = (1/M) \sum_{i=1}^{M} \delta\psi_i^2/2L_i$, where $\delta\psi_i$ is the flux step. The average is taken over M field lines with starting locations uniformly distributed over an unperturbed flux surface. Multiple field lines with a uniform poloidal angle interval on each flux surface are automatically traced for the first time to follow the lines with large elongation plasmas. The relation between diffusion coefficients is $\langle D_{\rm st} \rangle = C^2 r^2 \langle D_{\rm st}^{\psi} \rangle / 4\psi_i^2$. The conversion coefficient is $C = 0.83$–1.03 for the NSTX discharges. $C = 0.90$ is a reasonable approximation for edge plasma. The radial particle diffusion coefficient is calculated by $D_m = \langle D_{\rm st} \rangle \times C_{\rm s}$, where $C_{\rm s}$ is the ion acoustic speed. In contrast, the collisionless electron thermal diffusivity is defined as $\chi_e = \langle D_{\rm st} \rangle \times v_{T\rm e}$, where $v_{T\rm e} = \sqrt{T_{\rm e}/m_{\rm e}}$ is the thermal electron speed [7].

In NSTX, the EFIT equilibrium magnetic flux is specified on a 65×65 grid and a bi-cubic spline algorithm is used to evaluate the magnetic field between grid points. The initial radial position is replaced by the normalized magnetic flux. Multiple poloidal angles on the same magnetic flux surface are traced to produce a reasonably accurate approximation of the magnetic diffusion coefficient.

Two new subroutines were added to the initial TRIP3D code to model the stochastic magnetic perturbation in NSTX. One is applied to describe the complex positions of RWMEF coils. The other is for the calculation of the stochastic magnetic field produced by the RWMEF currents. The boundary limitation conditions in the main program are matched to the requirements of NSTX. The NSTX version of the TRIP3D code has been carefully verified by another code called PROBE, used to calculate the value of the magnetic field from the RWMEF coils at any point in the computational domain.

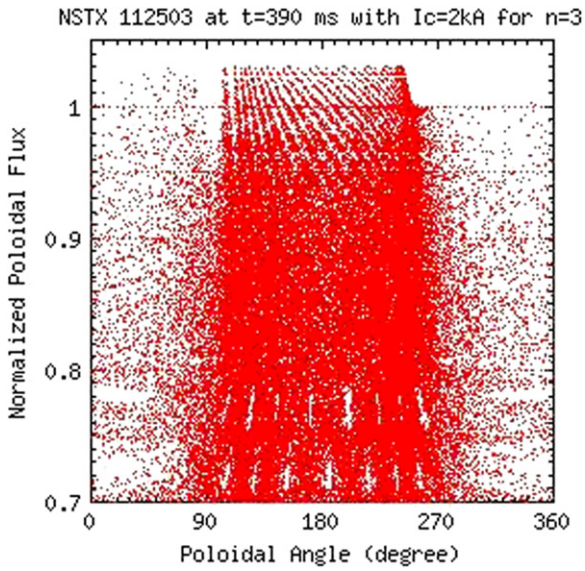

Figure 2. A Poincaré plot showing the positions of the field lines in terms of the normalized poloidal magnetic flux and poloidal angle with 0° at the outer NSTX midplane. The $m/n = 8/3$ mode located at $\psi_N = 0.72$ has a width of $\Delta\psi_N = 0.025$, while the $m/n = 9/3$ mode at $\psi_N = 0.775$ has a width of $\Delta\psi_N = 0.04$. There are 24 stripe-like structures between 100° and 250° on the top.

Up to now, the NSTX version of TRIP3D code is rather successful for simulating the stochastic magnetic boundary under various conditions.

3. The modelling results for stochastic magnetic boundary

Six RWMEF loops consist of either 18 or 22 line segments in the TRIP3D code. The perturbation vector field from each segment at each point along a field line trajectory is calculated using a Biot–Savart algorithm [8]. The toroidal modes are chosen as $n = 1$ or 3. Two divertor discharges are simulated to understand the difference between lower single null (LSN) and double null (DN) configurations.

Figure 2 shows the field line positions for normalized magnetic flux versus poloidal angle for LSN divertor discharge 112503 at $t = 390$ ms with the RWMEF current of $I_c = 2$ kAt and $n = 3$. The main parameters are $R = 0.85$ m, $a = 0.60$ m, $B_t = 0.44$ T, $I_p = 0.80$ MA, elongation $k = 2.07$, $\beta_t = 17\%$, $\beta_N = 5.4$, $\beta_p = 1.0$, safety factor $q_{95} = 6.1$ and $q_a = 12$. There are 72 field lines traced starting from a uniform poloidal distribution of 5° on each magnetic surface. Field lines are followed from each magnetic surface between $\psi_N = 0.7$ and $\psi_N = 1.0$ with the step of $\Delta\psi_N = 0.05$. Each field line is followed for 200 toroidal revolutions or until it intercepts the wall. The maximum length drops significantly from magnetic axis to the separatrix because (1) field lines are lost to the divertor and (2) the field lines reside predominantly on the high field side (HFS) in a spherical tokamak such as NSTX which reduces their length with increasing minor radius. The maximum length of a field line is about 1200 m at $\psi_N = 0.7$ and only 400 m at $\psi_N = 0.95$ after 200 toroidal revolutions, which is much larger than collisional mean free path (L_c). For example, using $T_{e,95} = 0.5$ keV, $n_{e,95} = 1.0 \times 10^{19}$ m^{-3}, we find $L_{c,95} = 54$ m. An $m/n = 6/3$ mode is observed at

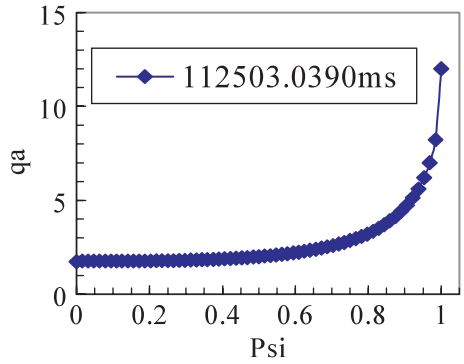

Figure 3. Safety factor profile versus normalized poloidal flux for shot 112503 at $t = 390$ ms in NSTX.

the $\psi_N = 0.50$ flux surface with the width of $\Delta\psi_N = 0.10$. This mode is not displayed in figure 2 because here we focus on the properties of the stochastic magnetic boundary. The $m/n = 8/3$ mode located at $\psi_N = 0.72$ has a width of $\Delta\psi_N = 0.025$, while the $m/n = 9/3$ mode at $\psi_N = 0.775$ has a width of $\Delta\psi_N = 0.04$. Field lines occupy almost the entire space except near island regions even with the step of $\Delta\psi_N = 0.05$. Some field lines do not complete 200 revolutions when $\psi_N > 0.75$ before hitting the divertor. All the open field lines eventually hit on the lower divertor for the LSN discharge. There are 24 stripe-like structures between 100° and 250° on the top, which appear to be consistent with a splitting of the separatrix into a stable and unstable manifold [9–11] as expected due to the Hamiltonian structure of the system. We note that the data in figure 2 are obtained by integrating the field lines in the forward or so-called unstable direction. Similar calculations in which field lines are integrated in the reverse or stable direction yield stripe-like structures that also appear to be consistent with the expected Hamiltonian structure of the system.

Figure 3 presents the safety factor profile versus normalized poloidal flux for shot 112503 at $t = 390$ ms to understand the difference between a spherical tokamak and a normal one. The safety factor on axis is $q_0 = 1.74$, while the surface of $q = 2$ is at $\psi_N = 0.50$, which is in good agreement with the position of magnetic islands of mode 6/3 in figure 2.

Figure 4 illustrates the LSN divertor configuration for shot 112503 at $t = 390$ ms in NSTX, which is reconstructed by the EFIT code using experimental data. The positive direction of poloidal angle is counter-clockwise. Large elongation can be easily obtained in NSTX. Another difference from a normal tokamak is the quite large Shafranov shift for the LCFS, which is about 15 cm for shot 112503. The inner target for lower divertor is located at the poloidal angle of about $\theta = 240°$, which can be verified by the top manifold in figure 2.

In contrast, figure 5 gives the magnetic flux versus poloidal angle for the same conditions except mode $n = 1$. The $m/n = 3/1$ mode appears at the same position as shown in figure 2. There are only eight stripes on the top, which is in good agreement with the $n = 1$ mode. For the $n = 1$ case, some field lines hit the divertor in less than 200 toroidal revolutions when started with $\psi_N > 0.85$. This implies that the $n = 1$ stochasticity is smaller than $n = 3$. Figures 2 and 3 clearly indicate the existence of relatively large stochastic deviations (of order 2% in $\Delta\psi_N$) from the unperturbed flux

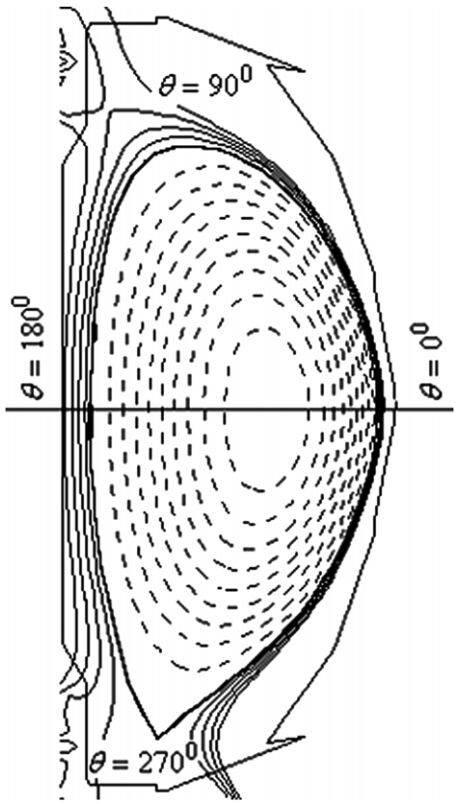

Figure 4. The LSN divertor configuration for shot 112503 at $t = 390$ ms in NSTX.

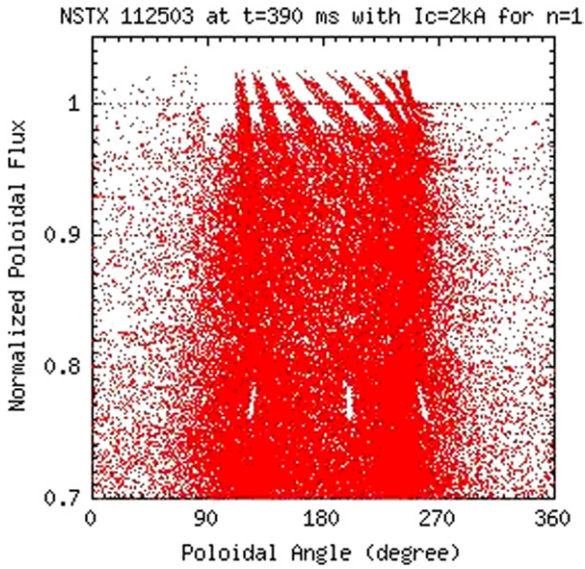

Figure 5. Magnetic flux versus poloidal angle for LSN shot 112503 at $t = 390$ ms with $I_c = 2$ kAt and mode $n = 1$. The $m/n = 3/1$ mode appears at the same position as shown in figure 2. There are only eight stripes on the top.

surface for $\psi_N > 1.0$ and poloidal angles between the outboard midplane at 0° and the top at 90°. These deviations also appear to be consistent with the Hamiltonian structure of the field lines previously seen in large aspect ratio poloidally diverted tokamaks [9–11]. The lack of points for $\psi_N > 1.0$ and poloidal angle $\theta \gtrsim 270°$ is due to the fact that the field lines were followed in only one toroidal direction and are swept to the wall at the divertor strike point.

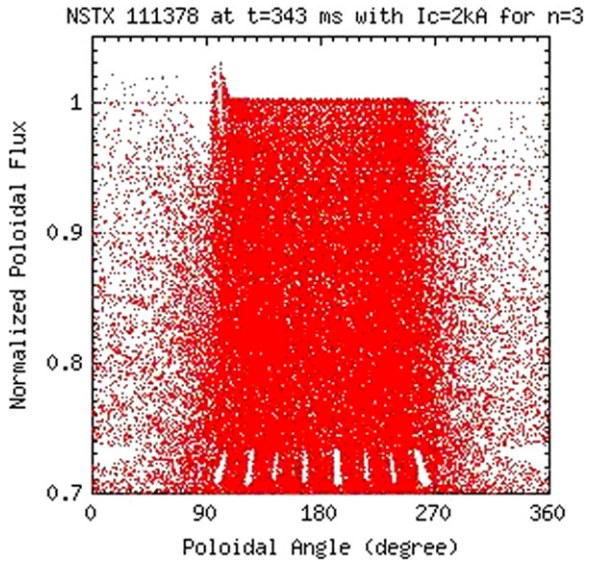

Figure 6. Magnetic flux versus poloidal angle for DN shot 111378 at $t = 343$ ms with $I_c = 2$ kAt and mode $n = 3$. The 9/3 mode appears at $\psi_N = 0.725$ because the safety factor in 111378 is higher than in 112503.

The magnetic flux versus poloidal angle for a DN divertor discharge 111378 at $t = 343$ ms with $I_c = 2$ kAt and an $n = 3$ perturbation is given in figure 6. The main parameters are $R = 0.85$ m, $a = 0.63$ m, $B_t = 0.44$ T, $I_p = 0.49$ MA, elongation $k = 1.87$, $\beta_t = 5.5\%$, $\beta_N = 3.1$, $\beta_p = 0.88$, safety factor $q_{95} = 9.7$ and $q_a = 31$. All the modelling conditions are similar to those in figure 2. The 9/3 mode appears at $\psi_N = 0.725$ because the safety factor in 111378 is higher than in 112503. Strong stochasticity is also observed in edge plasma but the stripe-like structures on the top have almost disappeared in the DN configuration. This may result because open field lines are now swept to the wall at the upper divertor. Additional calculations of the properties of the manifolds are needed to better understand this difference in the stripe-like structures. In the DN configuration some field lines hit the divertor before making 200 revolutions when starting with $\psi_N > 0.75$. The stochastic field difference between LSN and DN divertor discharges is small except for the top stripes and the way the field lines are lost, as shown in figures 2 and 6.

Figure 7 shows the stochastic magnetic diffusion coefficient $\langle D_{st} \rangle$ versus normalized flux for shot 112503 at $t = 390$ ms with the RWMEF-coil current of 2 kAt. There are 180 field lines traced on each magnetic flux surface and the step size in normalized magnetic flux is 0.01. The $\langle D_{st} \rangle$ of long path integrals tends to decrease with magnetic flux except near the magnetic island regions such as modes $m/n = 8/3$ at $\psi_N = 0.72$ and 9/3 at $\psi_N = 0.78$. The drop of the D_{st} in boundary plasma is caused by the field line hitting on the divertor target, (i.e. the domain available in $\delta\psi_i^2$ drops faster than L_i, the field line length, so $\langle D_{st}^{\psi} \rangle = (1/M) \sum_{i=1}^{M} \delta\psi_i^2 / 2L_i$ drops near the edge) where parallel transport along the magnetic field line gradually becomes the dominant process [12]. In contrast, the 3D transport simulations in stellarator W7-AS illustrates that the weight of the parallel transport in the island divertor geometry is substantially reduced in favour of the cross-field transport by the small field-line pitch and plasma-to-target distance [13]. The magnetic field structure in

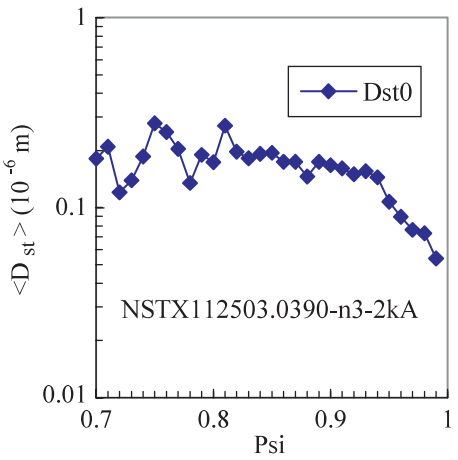

Figure 7. Stochastic magnetic diffusion coefficient versus normalized flux surface for shot 112503 with the current $I_c = 2$ kAt. The diffusion coefficient of long path integrals tends to decrease with magnetic flux in the edge.

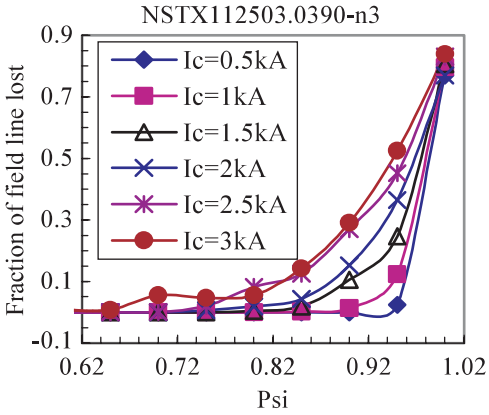

Figure 8. Normalized field line loss versus normalized magnetic flux for shot 112503 by different RWMEF-coil currents with mode $n = 3$. About 2.0 kAt current is necessary to produce a stochastic layer loss fraction comparable to that in DIII-D during the $n = 3$ I-coil ELM suppression experiments.

the peripheral region of the large helical device (LHD) was studied numerically with high accuracy [14]. It has been confirmed that low temperature ambient plasma is always present in the LHD chaotic field line layer outside the LCFS because of the very long connection length of the chaotic-field-line and the mirror confinement effect of the helical ripple nature of the LHD magnetic field. The coefficient at $\psi_N = 0.95$ is $\langle D_{st} \rangle = 1.07 \times 10^{-7}$ m. The radial particle diffusion coefficient is $D_m = 0.038\,m^2\,s^{-1}$ using $C_s = \sqrt{(T_e + T_i)/m_i} = 3.52 \times 10^5\,m^{-1}$ with $T_{e,95} = 0.5$ keV and $T_{i,95} = 0.8$ keV, while the collisionless electron thermal diffusivity is $\chi_e = 1.0\,m^2\,s^{-1}$. Based on experience from the DIII-D ELM suppression experiments [15], it appears that below 2 kAt the stochasticity may be too weak to have a significant effect on large ELMs.

The magnetic diffusion coefficient at $\psi_N = 0.95$ is $\langle D_{st} \rangle = 1.33 \times 10^{-7}$ m for shot 111378 at $t = 343$ ms with the DN divertor configuration. The radial diffusion coefficient is $D_m = 0.047\,m^2\,s^{-1}$ using $C_s = 3.52 \times 10^5\,m\,s^{-1}$ with $T_{e,95} = 0.5$ keV and $T_{i,95} = 0.8$ keV, while electron thermal diffusivity is $\chi_e = 1.25\,m^2\,s^{-1}$. For comparison, a simple method applied for the estimation of the thermal diffusivity in DIII-D gives $\chi_e = 0.9\,m^2\,s^{-1}$ with the C-coil current of 8 kAt [5]. Therefore, the stochastic field in NSTX is comparable to that in DIII-D when the NSTX coil is operated with about 25% of the current used in the DIII-D C-coil. The reason is that the magnetic field ratio in NSTX and DIII-D is about 1/4.

Shown in figure 8 is the fraction of field lines lost versus normalized magnetic flux for shot 112503 with different RWMEF currents and an $n = 3$ perturbation. Six RWMEF currents are given, for example $I_c = 0.5$, 1.0, 1.5, 2.0, 2.5 and 3.0 kAt. No loss means that all trace field lines remain inside $\psi_N = 1.0$ after 200 toroidal revolutions. There is an obvious loss from $\psi_N = 0.70$ when using RWMEF current of 3 kAt. A small loss appears at $\psi_N = 0.95$ with the RWMEF current of 0.5 kAt. Thus, the data indicate a minimum RWMEF current of about 2.0 kAt is necessary to produce a stochastic layer loss fraction comparable to that in DIII-D during the $n = 3$ I-coil ELM suppression experiments although the properties of the stochastic layer (number of islands across the pedestal and their widths) are significantly different with the I-coil in DIII-D [15]. The results illustrate that the RWMEF design capability of 6 kAt in NSTX is rather large to produce the stochastic field for the ELM control. Initial experiments in NSTX indicate that a minimum RWMEF current of 2 kAt is needed to begin observing small, irreproducible, effects on the ELM behaviour. This suggests that experiments at higher RWMEF current should have a clear and reproducible effect on ELMs in NSTX and appears to agree quite well with the coil current threshold predicted by our modelling results.

4. Conclusions

The new version of three-dimensional TRIP3D code [5] has been successfully applied to model stochastic magnetic perturbation with toroidal mode $n = 1$ or 3 produced by RWMEF-coil currents in NSTX with very low aspect ratio for the first time. The edge stochastic fields with LSN divertor for shot 112503 and DN divertor for shot 111378 are simulated by the code. Since the RWMEF-coil is closer to the plasma than the DIII-D C-coil and the magnetic field B_t is about a factor of four lower in NSTX, the NSTX coil requires only 25% of the current needed in the DIII-D C-coil to produce an equivalent stochastic layer. Many magnetic islands are produced at different rational magnetic surfaces with sufficient RWMEF currents. The stochastic field strongly depends on the RWMEF current and is almost independent of divertor configuration.

The field line loss caused by the stochastic field and level of stochastic diffusivity indicates that a minimum RWMEF-coil current of about 2 kAt is needed to affect large ELMs in NSTX. The results illustrate that the RWMEF design capability of 6 kAt in NSTX is rather large to produce the stochastic field for ELM control. Initial experiments in NSTX indicate that an RWMEF current of 2 kAt begins to have a weak, irreproducible effect on the ELM behaviour suggesting that 2 kAt is close to the stochastic magnetic field diffusion threshold, predicted by our modelling results, for good ELM suppression. In NSTX the $n = 3$ field is more effective than the $n = 1$ field at the same current for producing a stochastic layer. The magnetic diffusion coefficient tends to decrease with normalized magnetic flux for the long path integrals over 200 toroidal revolutions. The magnetic diffusion coefficient

of edge plasma decreases with normalized magnetic flux. The reason is that the parallel transport along the magnetic field line gradually becomes the dominant process for the edge plasma. The radial particle diffusion coefficient at $\psi_N = 0.95$ is about $0.038\,m^2\,s^{-1}$ in the LSN and about $0.047\,m^2\,s^{-1}$ in the DN divertor if the RWMEF current of 2 kAt is used; the corresponding collisionless electron thermal diffusivity is $1.0\,m^2\,s^{-1}$ for LSN and $1.25\,m^2\,s^{-1}$ for the DN divertor.

Acknowledgments

This work was supported in part by the U.S Department of Energy under DE-FC02-04ER54698, DE-AC02-76CH03073 and DE-AC05-00OR22725 and by the Chinese Ministry of Science and Technology under grant No 001CB710904. The authors would like to thank Dr M. Schaffer at General Atomics for confirming the NSTX version of TRIP3D code with the PROBE code, Dr C. Wong for arranging the China/USA collaboration and Dr J. Menard for providing the NSTX RWMEF coil coordinates. This work was supported by fusion collaboration between China and the USA on fluid plasma simulation.

References

[1] Ono M. *et al* 2000 *Nucl. Fusion* **40** 557
[2] Kaye S.M. *et al* 2003 *Phys. Plasmas* **10** 3953
[3] Maingi R. *et al* 2005 *Nucl. Fusion* **45** 1066
[4] Scoville J.T. and La Haye R.J. 1991 *Proc. 14th IEE/NPSS Symp. on Fusion Engineering (San Diego, USA)* vol 2 (Piscataway, NJ: Institute of Electrical and Electronics Engineers, Inc) p 1144
[5] Evans T.E., Moyer R.A. and Monat P. 2003 *Phys. Plasmas* **9** 4957
[6] Lao L.L. *et al* 2005 *Fusion Sci. Technol.* **48** 968
[7] Rechester A.B. and Rosenbluth M.N. 1978 *Phys. Rev. Lett.* **40** 38
[8] Hanson J.D. and Hirshman S.P. 2002 *Phys. Plasmas* **9** 4410
[9] Evans T.E. *et al* 2005 *J. Phys.: Conf. Ser.* **7** 174
[10] Roeder R.K.W., Rapoport B.I. and Evans T.E. 2003 *Phys. Plasmas* **10** 3796
[11] Abdullaev S.S., Finken K.H., Jakubowski M. and Lehnen M. 2006 *Nucl. Fusion* **46** S113.
[12] Ghendrih Ph. *et al* 2002 *Nucl. Fusion* **42** 1221
[13] Feng Y. *et al* 2002 *Plasma Phys. Control. Fusion* **44** 611
[14] Watanabe T. *et al* 2006 *Nucl. Fusion* **46** 291
[15] Evans T.E., Moyer R.A., Thomas P.R. 2004 *Phys. Rev. Lett.* **92** 235003-1